PN admittance characterisation of grid supporting VSC controllers with negative sequence regulation and inertia emulation

Callum Henderson[1], Lie Xu[1], Agusti Egea-Alvarez[1]

[1] Power Electronics, Drives and Energy Conversion Group, Electronic and Electrical Engineering Department, University of Strathclyde, Glasgow, Scotland
Tel.: 0141 552 4400
E-Mail: Callum.Henderson.100@strath.ac.uk

Acknowledgements

The first author would like to acknowledge support from the Engineering and Physical Sciences Research Council, Grant Number: EP/R513349/1

Keywords

Impedance Analysis, Synthetic Inertia, Droop Control, Grid-connected converter, Converter control

Abstract

This work presents an analysis of converter output admittance for grid supporting VSC controllers in the positive – negative frame (pn-frame). Previously discovered issues in other reference frames are explored to prove the efficacy of analysis in the pn-frame The effect of negative sequence control is often overlooked and the pn-frame offers a useful method for observing the result. The impact of control parameters such as PLL bandwidth was explored which decreased network damping and increased regions of negative incremental impedance. Reduction of unwanted admittance components was achieved by the addition of appropriately tuned voltage feedforward filters. The equivalence of inertia and droops has been documented previously but not utilising converter impedance. Analogous traces of impedances were obtained for each structure with a similar response obtained when changing the respective associated gain indicating an equivalence.

Introduction

Power converter interfaced generation is becoming increasingly popular due to a shift from traditional fossil fuel generators to cleaner renewable energy sources. This has been largely driven by strategy and policy to combat climate change [1]. As example, in the UK, the electricity network has seen 35.8 % of hydrocarbon based power stations replaced with renewable energy sources by 2019 [2]. While the move to renewable energy is extremely important, the introduction of more power converters to the electricity network leads to new challenges in maintaining network stability and control. Having large, heavy spinning masses connected to the network is beneficial as they provide significant damping and inertia to smooth large power deviations. The UK network may see as large as 40 % reduction in inertia by 2025 [3]. Traditional generators are extremely robust and help to support the grid during faults and network events. As these generators are taken offline new challenges emerge to maintain stability in a converter dominated network [4].

Conventional converter current control provides little useful behaviour in terms of stability and reduces network strength in locations where it is utilised due to reduced fault current and voltage damping [5]. The family of controllers that use a PLL or similar synchronisation loop are known as grid following controllers as they ‘follow’ a pre-existing voltage signal. The simple current controller can be augmented with outer loop controllers to enhance grid support by providing services such as inertia and reactive power support [6, 7]. It has been reported that PLL performance is reduced in low inertia grids due to increased frequency variations and the susceptibility of the PLL to signal noise [8]. In addition, the tuning can largely effect converter output impedance and therefore efforts to retune the PLL to improve performance in certain situations could harm stability overall [9]. Negative sequence control (NSC) is utilised to cope with unbalanced grid conditions mainly during faults but the controller is usually active during normal operation to cope with small voltage imbalances. The addition of negative sequence

This is a peer-reviewed, accepted author manuscript of the following paper: Henderson, C., Xu, L., & Egea Alvarez, A. (2021). PN admittance characterisation of grid supporting VSC controller with negative sequence regulation and inertia emulation. Paper presented at 23rd European Conference on Power Electronics and Applications.

control significantly alters the converter impedance and can lead to stability concerns. Little literature exists surrounding the positive-negative (pn) frame. The ability to observe the decoupled positive and negative sequence is beneficial when considering different sequence controllers. One article completed by Amico et al. provides methods of obtaining the pn-frame impedance from the dq-frame [12]. The method described in [12] will be used in this work. Previously reported issues should be investigated in the pn-frame to verify the robustness of admittance analysis while exploring often overlooked control aspects such as NSC. This will provide characterisations aiding future work on determining stability via the impedance method.

Impedance or admittance based analysis has been used extensively in literature [10, 11]. It provides a method of studying interactions points and possible unwanted behaviour using easily measured quantities. Considerable work exists analysing the dq-frame looking at the effect of control gains and grid strength connection. A study conducted by Wen. et al. explored the effect of PLL tuning on dq-frame impedance and found that the PLL bandwidth significantly affected regions of negative incremental impedance (NII). New control structures are attempting to provide support to the grid via a frequency based command. The frequency estimation is provided via the PLL and will significantly affect the converter impedance. This paper aims to characterise the effects of negative sequence control, PLL tuning and control parameters on the pn-frame admittance for different grid supporting control structures using a traditional power voltage current controller for reference.

Controller Layouts

This section describes the control structures used for analysis. Each consists of an inner loop current controller fed from a power and voltage control scheme with a negative sequence current controller running parallel. Network synchronisation for each controller is provided via a phase-locked loop (PLL). A control diagram is provided for each followed by a description of the operation. The first structure, a traditional power voltage current controller with negative sequence control is shown in Figure 1 [12]. Two other grid following structures are investigated, the power voltage current controller with inertia emulation (PVCCI) [6], shown in Figure 2 and the power voltage current controller with droops (PVCCD) [7], illustrated in Figure 3. Only the outer control loops which provide the current references for the positive sequence current controller are shown in Figure 2 and Figure 3 as the remaining controller topology remains constant. Table I lists the controller abbreviations for clarity.

From Figure 1, the purple and red boxes show the positive and negative sequence current loops respectively, regulating the positive sequence currents $i_{cq,p}$ and $i_{cd,p}$ and the negative sequence currents $i_{cq,n}$ and $i_{cd,n}$. Where $K_{ic}(s)$ are PI controllers with tuneable bandwidths, ωL_f represents the cross coupling between the q and d axes and $U_{q,p}$, $U_{d,p}$, $U_{q,n}$ and $U_{d,n}$ are the positive and negative sequence q and d voltage feedforwards respectively. The outer loop, shown in green, regulates the active power flow by providing the positive q-axis current command via the PI controller represented by $K_{on,P}(s)$. The voltage magnitude at the PCC is maintained by generating a positive d-axis current command via the PI controller $K_{on,U}(s)$. A PLL (shown in light blue) provides synchronisation with the grid utilising a PI controller which acts on the positive sequence d-axis voltage. The processing system shown in dark blue includes two park transforms $T(\theta)$, with the positive sequence transform operating with positive PLL angle and the negative sequence being fed the negative PLL angle. Notch filters tuned at 100 Hz are applied to decouple the positive and negative sequence [12]. Before converter voltage generation, the negative sequence commands $v_{cdq,n}$ must be transferred back to the positive frame by applying a rotation of $e^{-2J\omega_0 t}$ contained within $T_N(\theta)$. In Figure 2, the green outer loop of the PVCCI is the same as in Figure 1. However, a frequency deviation based power command is added to provide inertia emulation. The function $K_{in}(s)$ consists of a derivative term to provide RoCoF, a smoothing filter and a tuneable gain to adjust the inertia response. The outer loop of the PVCCD shown in Figure 3 replaces the active power and PCC voltage PIs with P controllers to provide a droop.

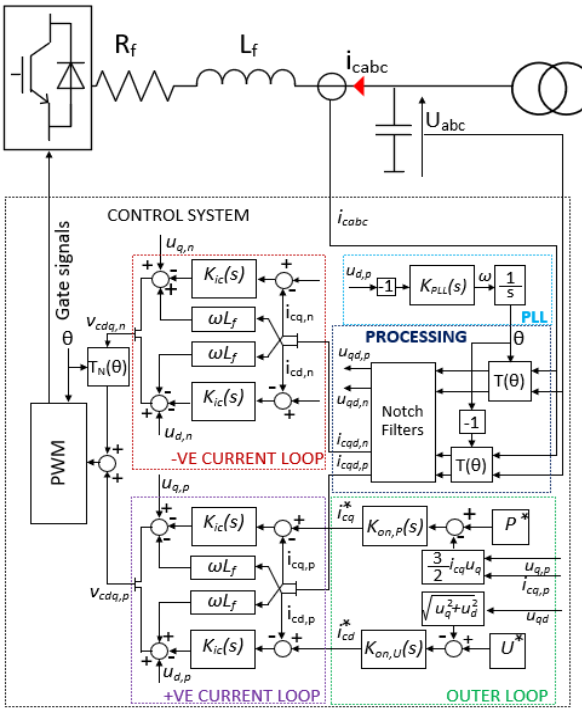

Figure 1 Power voltage current controller with negative sequence control (PVCCN)

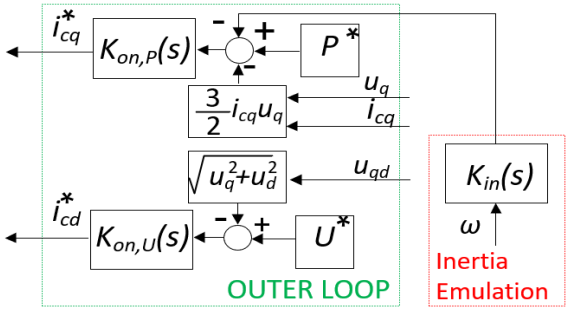

Figure 2 PVCCI outer control loop

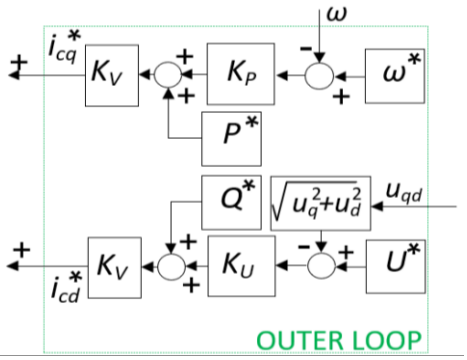

Figure 3 PVCCD Outer control loop

Table I List of Control Modes

Controller Description	Notation	Figure
Power Voltage with Positive/Negative Sequence Current Control	**PVCCN**	**1**
Power Voltage with Positive/Negative Sequence Current Control and Inertia Emulation	**PVCCIN**	**2**
Power Voltage Droops with Positive/Negative Sequence Current Control	**PVCCDN**	**3**

A linearised small-signal model was created for each control type in the positive dq-frame and all negative sequence control parameters were referred into the positive frame. In addition, the transformation described in [12] was used to convert the dq-frame impedance into the pn-frame. The small signal models were verified against frequency sweeps completed in time domain large signal models and the result is shown in Figure 4.

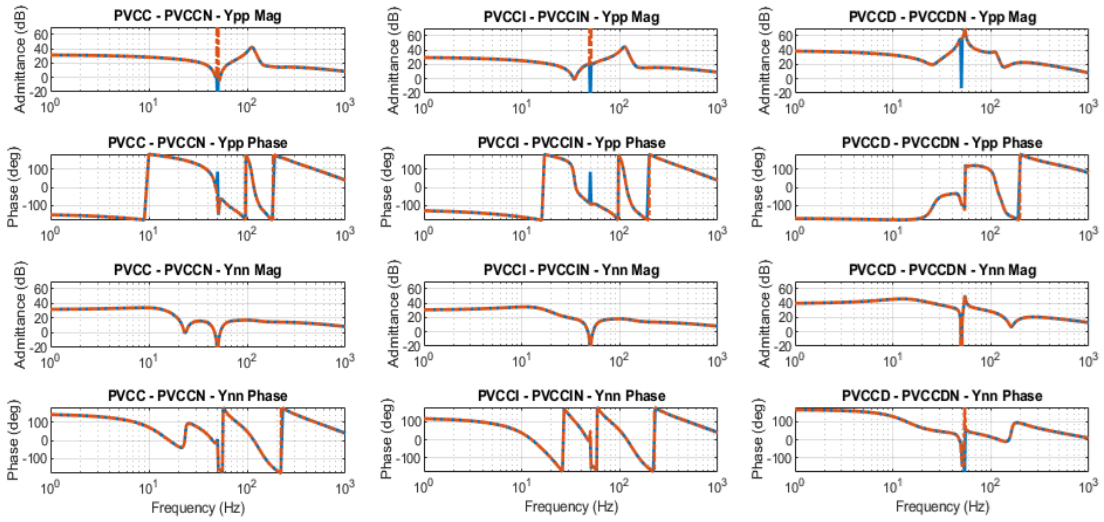

Figure 4 Small-signal model validations - Time domain response (blue solid) - Small-signal response (red dot-dash)

A strong agreement was achieved for all models throughout the range of analysed frequencies. There are discrepancies in each case at 50 Hz due to the response being undefined. The integral component of the voltage controller causes the theoretical response to grow to infinity and this is approximated in the models differently. The inter-sequence coupling components are not provided but exhibited a similar match to the signals provided. Double subscript notation is employed for the admittance indicating that Y_{PN} is the positive sequence response to a negative sequence injection and so forth. Only the positive-postive and negative-negative impedances are shown for verification in Figure 5, Figure 6 and Figure 7.

Comparison of Negative and Positive Sequence Control

In this section the converter output admittance in the pn-frame is compared for controllers with and without negative sequence control enabled. The comparisons for PVCC, PVCCI and PVCCD are shown in Figure 5, Figure 6 and Figure 7 respectively. PVCCN, PVCCIN and PVCCDN represent the same control structures with negative sequence control enabled.

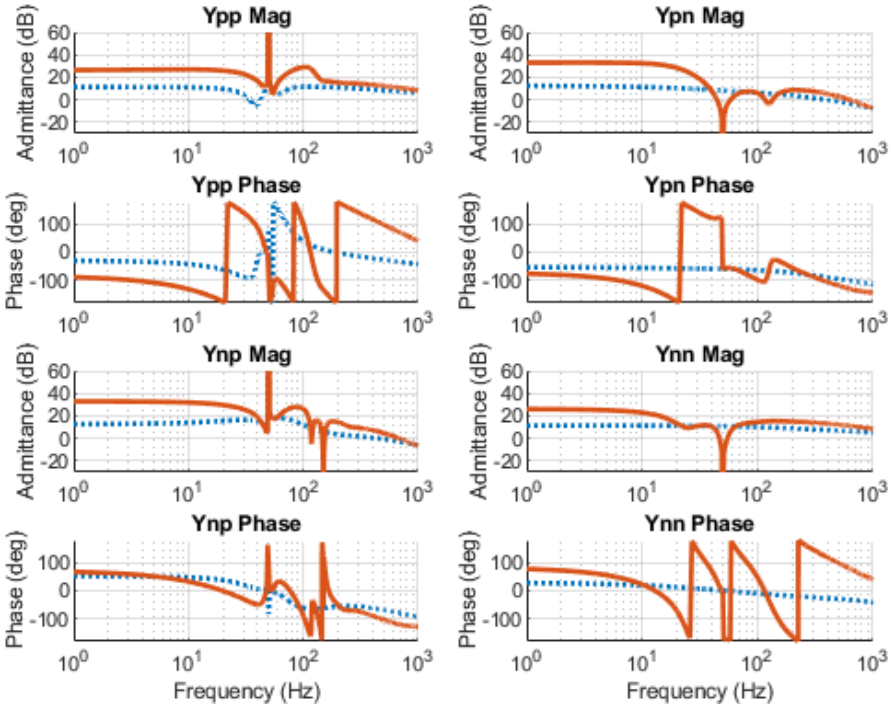

Figure 5 PVCC (blue dot) and PVCCN (orange solid) PN Y

From Figure 5, Figure 6 and Figure 7, when NSC is disconnected the converter reaction to a negative sequence injection represents that of an inductor with the admittance falling at high frequencies and the phase angle tending to -90°. The addition of NSC leads to increased converter admittance, reduced network damping for PVCCN and PVCCIN and increased regions of negative incremental impedance (NII) for all controllers. NII is defined as the regions where the admittance phase does not satisfy the condition - $(-90° < \angle Y < 90°)$. The PVCCN and PVCCIN converter admittance is similar with the addition of inertia emulation appearing to further reduce network damping. The DC admittance is larger when NSC is enabled with the largest difference observed with PVCCN. The addition of inertia emulation appears to remove the region of NII in the (50-90 Hz) that is present with the PVCCN. While regions of NII are increased when NSC is added to the droop controller, the admittance remains largely the same however greater damping can be observed in the negative sequence around 50 Hz.

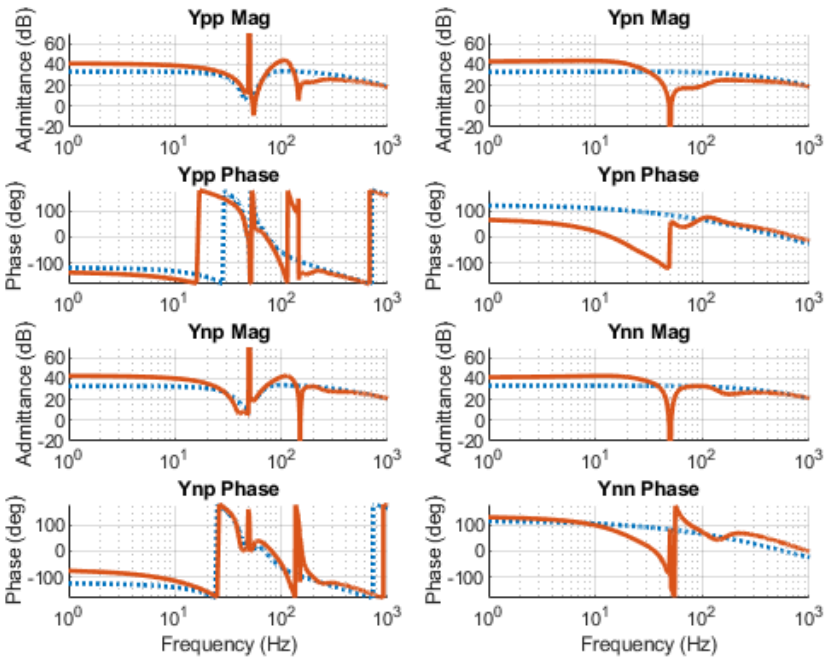

Figure 6 PVCCI (blue dot) and PVCCIN (orange solid) pn-admittance

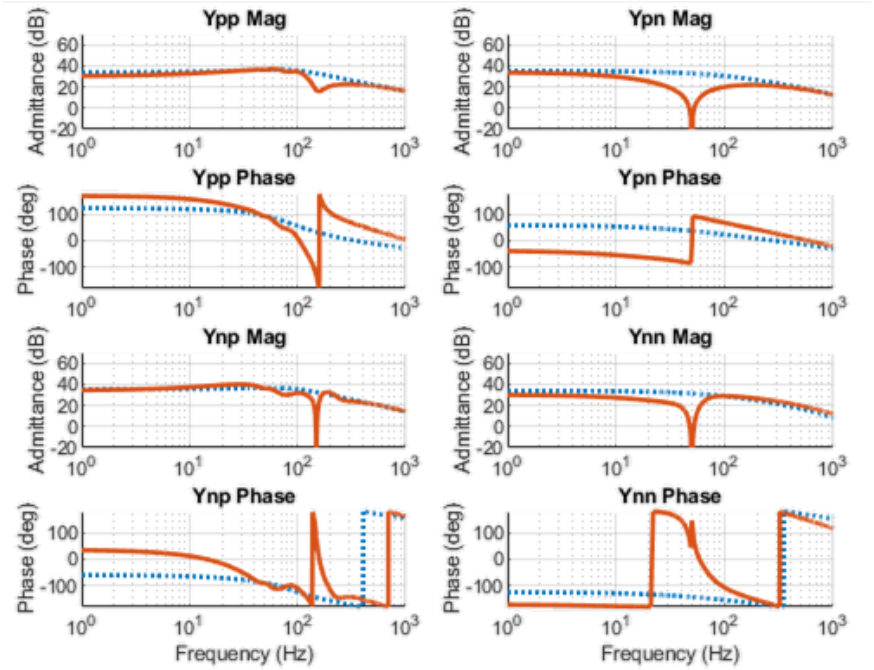

Figure 7 PVCCD (blue dot) and PVCCDN (orange solid) PN Y

PLL Impact

Research has been conducted exploring the effect of PLL bandwidth on the d or q-axis (dependent on frame alignment) impedance/admittance. These works have found that reduced PLL bandwidth can reduce areas where the converter behaves as negative incremental resistor and harm network stability [10, 11]. This section explores the effect in pn-frame. Figure 8, Figure 9 and Figure 10 illustrate the change in converter admittance for three PLL bandwidths for the PVCCN, PVCCIN and PVCCDN respectively.

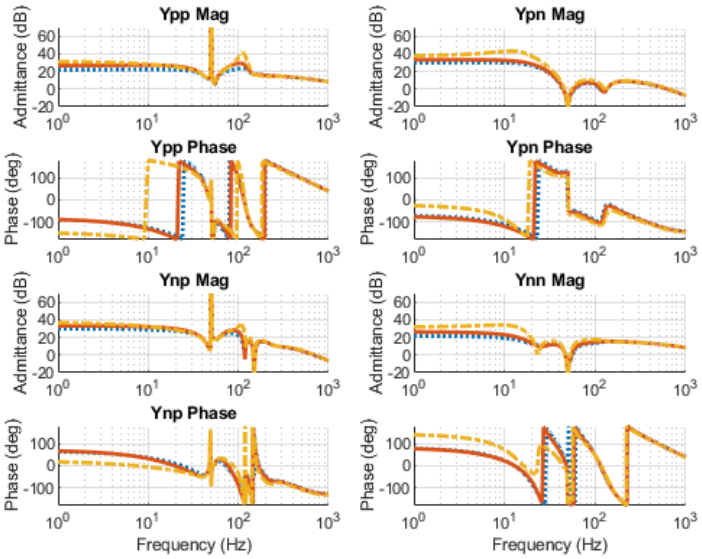

Figure 8 PLL BW effect on PVCCN (blue dot -300 Hz)(orange solid – 400 Hz)(yellow dash – 500 Hz)

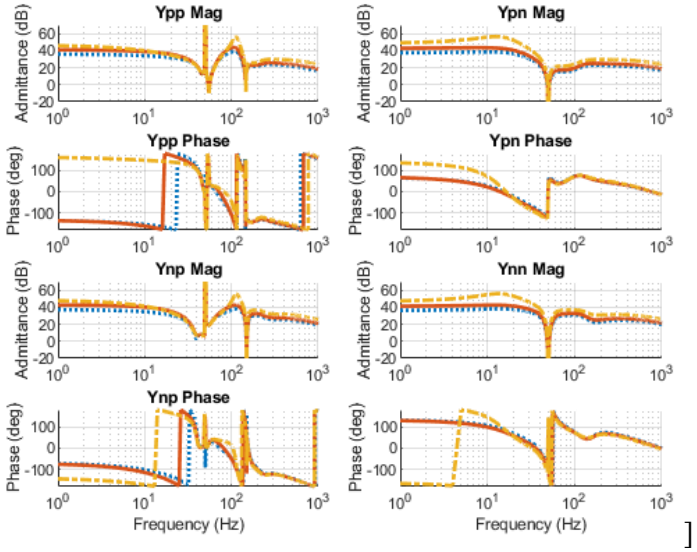

]

Figure 9 PLL BW effect on PVCCIN (blue dot -300 Hz)(orange solid – 400 Hz)(yellow dash – 500 Hz)

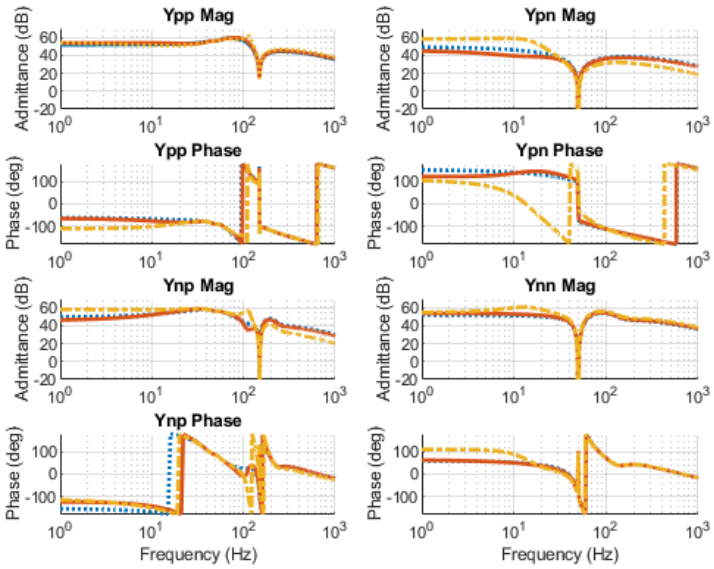

Figure 10 PLL BW effect on PVCCDN (blue dot -300 Hz)(orange solid –400 Hz)(yellow dash –500 Hz)

From Figure 8, the region of NII is increased with a higher PLL bandwidth which is consistent with findings made by Wen et al [11]. However in Figure 9, it can be seen that when inertia emulation is used that the increased PLL bandwidth reduces the width of the NII for frequency ranges where the PVCCN exhibited an increase. The effect on the PVCCDN shown in Figure 10 is small with no significant differences observed in the cases of NII. However, in all controllers increased PLL bandwidth led to reduced network damping. In the case of the supporting control structures the effect of PLL bandwidth can be exacerbated by increasing the frequency control gain. This indicates that the addition of structures to support the grid will provide challenges in tuning to ensure stable operation. The benefits provided to the grid do not come without consequence.

Reduction of NII Using Voltage Feedforward Filters

Previous studies have concluded that the voltage feedforward (VFF) terms in the inner loop current control greatly influence converter impedance [13]. By applying low-pass filters (LPFs) to the VFF terms in the positive and negative sequence regions of NII can be reduced and inspection of the pn-frame impedances shows this clearly. Utilising the PVCCN, low-pass filters tuned with a time constant (τ_{VFF}) are implemented and a comparison of the admittance is shown in Figure 11.

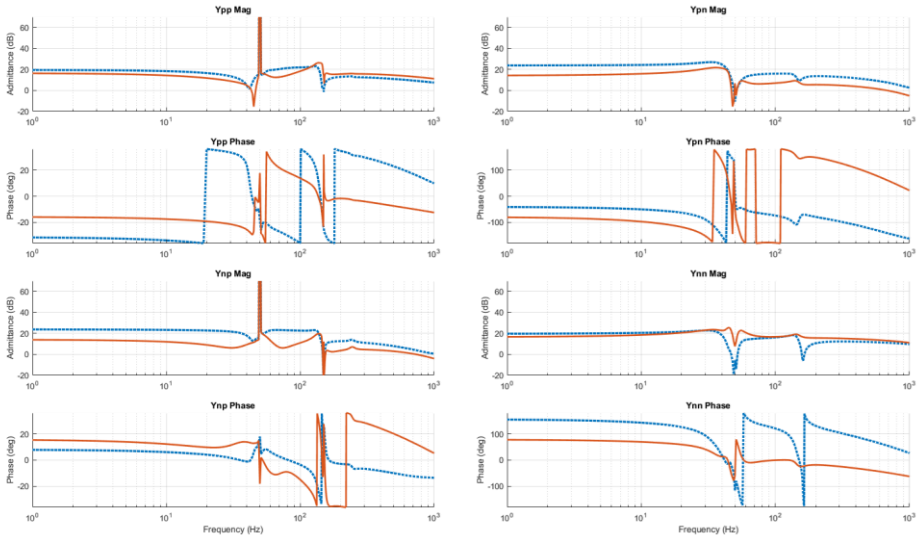

Figure 11 Comparison of pn-frame admittance for PVCCN without VFF (blue dot) and with VFF (orange solid)

From Figure 11, it can be seen the addition of the LPF completely removes any regions of NII from the negative sequence and provides a significant reduction in the positive sequence. The overall damping of the system is improved slightly. These improvements lead to increased stability of the system. When right-hand-plane (RHP) zeros are present in the admittance transfer function it is an indication of NII [14]. This is easy to see in the Y_{nn} trace in Figure 11 at around 180 Hz, the phase jump and large dip in the blue dot trace indicates a RHP zero. When the LPF is introduced the RHP is removed and the region of NII is vastly reduced. The time constant can be tuned to further improve the response. The PVCCN admittance is shown for three time constants in Figure 12. Figure 12 indicates that the positive sequence impedance is the most sensitive to variations in filter time constant. The best response is observed for $\tau_{VFF} = 30\ ms$ as the smallest region of NII is observed. A smaller time constant slightly reduces the NII below 50 Hz but a large increase is observed above 50 Hz. The opposite effect occurs for a larger time constant. The 90° phase jump and large anti-resonance around 45 Hz when $\tau_{VFF} = 50\ ms$ indicates the presence of a RHP zero. By decreasing the filter time constant the zero is shifted from the RHP and a reduction in NII is observed improving overall stability.

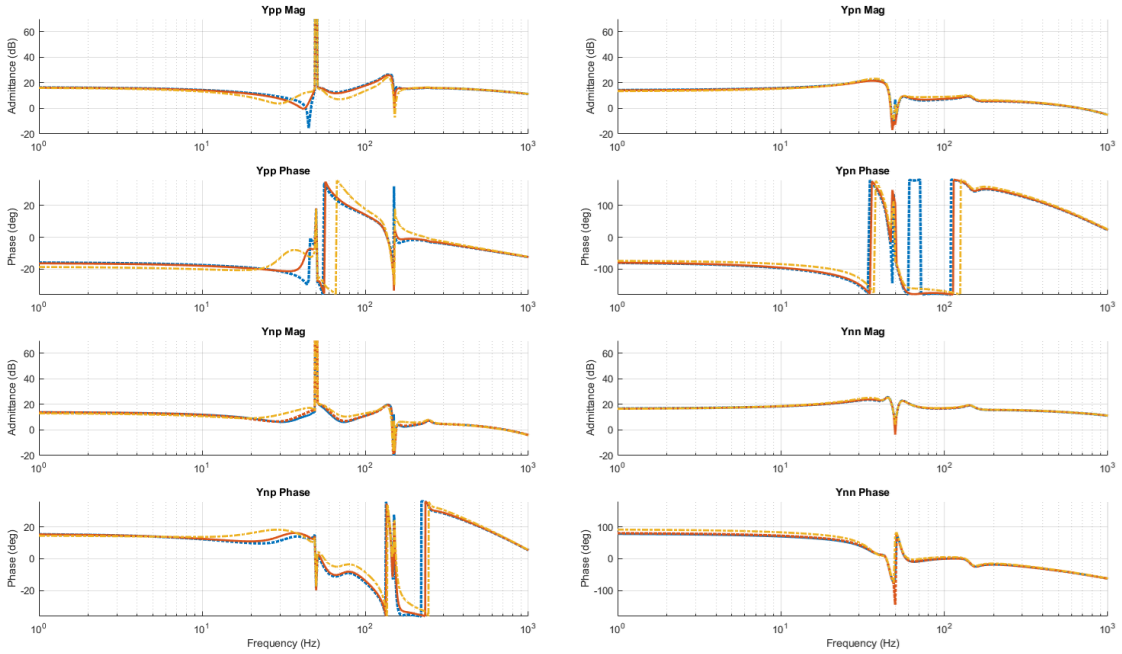

Figure 12 Effect of VFF LPF time constant on PVCCN admittance ($\tau_{VFF} = 50\ ms$ – blue dot) ($\tau_{VFF} = 30\ ms$ – orange solid) ($\tau_{VFF} = 10\ ms$ – yellow dash)

Equivalences of Droops and Inertia

Some studies have discussed equivalences between droop control and virtual inertia [15]. In this section, the inertial gain of the PVCCIN, shown in Figure 11 and the frequency droop gain of the PVCCDN, shown in Figure 12 is varied to analyse the effect on the converter admittance. A comparison of the responses is provided in Table II. The response is measured between the onset of the frequency deviation to 90 % of the final-steady state power. The droop gain was set to provide the percentage droops shown in Table 2 and the inertial gain was tuned to provide a similar peak power response. From Figure 11 and Figure 12, the change in converter admittance for a change in the respective frequency control gain is very similar - the system damping is reduced as the gain increases. The droop gain remedies the regions of NII with the PVCCDN slightly better than the inertial gain with the PVCCIN. The largest response achieved was around 410 kW to a 1 $rads^{-1}$ event for both controllers. The response with inertia emulation is faster than when droop control is employed.

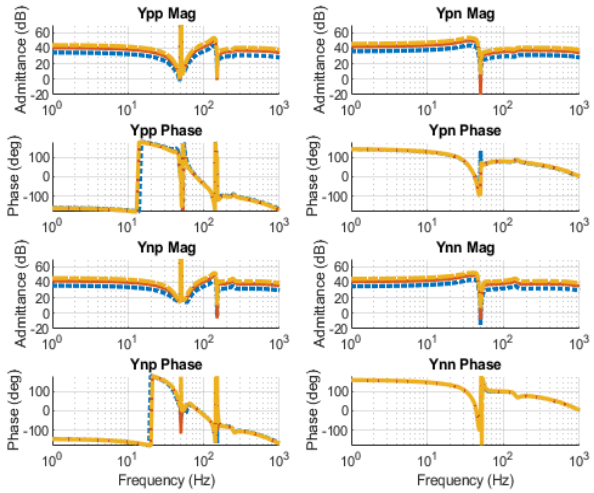

Figure 13Effect of inertia gain on PVCCIN Y (legend shown in Table 1)

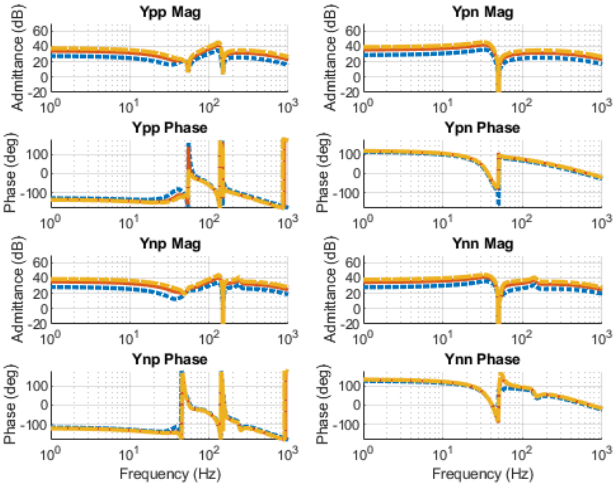

Figure 14 Effect of frequency droop gain on PVCCDN Y (legend shown in Table 1)

With traditional control, the addition of frequency support should not greatly affect the admittance. However, in these cases the PLL dynamics are amplified by the inertial or droop gain and the current command is directly impacted by the provided frequency deviation. If it assumed that a higher converter admittance is preferable to avoid interactions with a high impedance (low SCR grid) then it may be preferable to tune the inertial/droop gains higher in weaker grids and lower in stronger to improve stability. However, care must be taken with the reduction in system damping that will occur.

Table II Peak frequency response of PVCCIN and PVCCDN for different control gains

PVCCIN				**PVCCDN**			
Inertia Gain Value (K_{inert})	**Peak Power Response**	**Response Time**	**Trace - Figure 11**	**Droop Gain Value (K_wD)**	**Peak Power Response**	**Response Time**	**Trace – Figure 12**
15000	120 kW	7 ms	Blue dotted	$1x\ 10^5$ (8 % droop)	120 kW	12 ms	Blue dotted
27500	230 kW	7 ms	Orange solid	$2x10^5$ (4 % droop)	230 kW	12 ms	Orange solid
41000	350 kW	7 ms	Yellow dash	$3x10^5$ (3 % droop)	350 kW	12 ms	Yellow dash

Conclusion

The converter output admittance in the PN frame for three grid following control structures has been explored. The effect of negative sequence control significantly increased converter admittance and therefore reduced network damping. In addition, NSC increased regions of negative incremental impedance for all control structures. The bandwidth of the PLL was found to significantly impact regions of NII for all control types. For traditional control this matched previous studies conducted in the dq-frame. However, it was found that the addition of inertia emulation allowed a reduction in the width of some regions of NII but this was only necessary due to the addition of NSC. The best method of reducing NII regions was to appropriately filter feedback voltages before adding them to the positive and negative sequence control. When comparing the grid supporting capabilities of inertia emulation and droop control, the pn-frame admittance for both control types exhibited similar sensitivity to the respective control frequency gain. This indicates an equivalence and may negate the need for the added complexity of inertia emulation over droop control.

References

[1] Department for Business Energy & Industrial Strategy, "UK National Energy and Climate Plan (NECP)," presented at the UK government, London, 2019.

[2] E. I. S. Department for Business, "UK Energy Statistics, Q1 2019," *Statistical Press Release,* 2019.

[3] National Grid ESO. "Operating a Low Inertia System - A System Operability Framework Document." https://www.nationalgrideso.com/document/164586/download (accessed Aug, 2020).

[4] H. Urdal, R. Ierna, and A. J. Roscoe, "Stability challenges & solutions for power systems operating close to 100% penetration of power electronic interfaced power sources: exchange of experience between hybrid and major power systems," *3rd International Hybrid Power Systems Workshop,* 2018.

[5] EnTSO-E, "High Penetration of Power Electronic Interfaced Power Sources and the Potential Contribution of Grid Forming Converters," Brussels, 2020.

[6] J. Morren, S. W. H. De Haan, W. L. Kling, and J. A. Ferreira, "Wind Turbines Emulating Inertia and Supporting Primary Frequency Control," *IEEE Transactions on Power Systems,* vol. 21, no. 1, pp. 433-434, 2006, doi: 10.1109/tpwrs.2005.861956.

[7] J. Rocabert, A. Luna, F. Blaabjerg, and P. Rodríguez, "Control of Power Converters in AC Microgrids," *IEEE Transactions on Power Electronics,* vol. 27, no. 11, pp. 4734-4749, 2012, doi: 10.1109/tpel.2012.2199334.

[8] F. Milano, F. Dörfler, G. Hug, D. J. Hill, and G. Verbič, "Foundations and Challenges of Low-Inertia Systems (Invited Paper)," in *2018 Power Systems Computation Conference (PSCC)*, 11-15 June 2018 2018, pp. 1-25, doi: 10.23919/PSCC.2018.8450880.

[9] X. Wang, L. Harnefors, and F. Blaabjerg, "Unified Impedance Model of Grid-Connected Voltage-Source Converters," *IEEE Transactions on Power Electronics,* vol. 33, no. 2, pp. 1775-1787, 2018, doi: 10.1109/TPEL.2017.2684906.

[10] B. Wen, D. Boroyevich, P. Mattavelli, R. Burgos, and Z. Shen, "Modeling the output impedance negative incremental resistance behavior of grid-tied inverters," 2014 2014: IEEE, doi: 10.1109/apec.2014.6803550. [Online]. Available: https://dx.doi.org/10.1109/apec.2014.6803550

[11] B. Wen, D. Boroyevich, R. Burgos, P. Mattavelli, and Z. Shen, "Analysis of D-Q Small-Signal Impedance of Grid-Tied Inverters," *IEEE Transactions on Power Electronics,* vol. 31, no. 1, pp. 675-687, 2016, doi: 10.1109/tpel.2015.2398192.

[12] G. Amico, A. Egea-Alvarez, P. Brogan, and S. Zhang, "Small-Signal Converter Admittance in the pn-Frame: Systematic Derivation and Analysis of the Cross-Coupling Terms," *IEEE Transactions on Energy Conversion,* vol. 34, no. 4, pp. 1829-1838, 2019, doi: 10.1109/tec.2019.2924922.

[13] J. Wang, J. Yao, H. Hu, Y. Xing, X. He, and K. Sun, "Impedance-based stability analysis of single-phase inverter connected to weak grid with voltage feed-forward control," 2016 2016: IEEE, doi: 10.1109/apec.2016.7468169. [Online]. Available: https://dx.doi.org/10.1109/apec.2016.7468169

[14] X. Wang, F. Blaabjerg, and P. C. Loh, "An impedance-based stability analysis method for paralleled voltage source converters," 2014 2014: IEEE, doi: 10.1109/ipec.2014.6869788. [Online]. Available: https://dx.doi.org/10.1109/ipec.2014.6869788

[15] S. D. Arco and J. A. Suul, "Virtual synchronous machines — Classification of implementations and analysis of equivalence to droop controllers for microgrids," in *2013 IEEE Grenoble Conference*, 16-20 June 2013 2013, pp. 1-7, doi: 10.1109/PTC.2013.6652456.